ISSN 1063-7850, Technical Physics Letters, 2020, Vol. 46, No. 5, pp. 442–445. © Pleiades Publishing, Ltd., 2020.
Russian Text © The Author(s), 2020, published in Pis'ma v Zhurnal Tekhnicheskoi Fiziki, 2020, Vol. 46, No. 9, pp. 35–38.

Heterostructures of Quantum-Cascade Laser for the Spectral Range of 4.6 μm for Obtaining a Continuous-Wave Lasing Mode

A. V. Babichev[a]*, A. G. Gladyshev[a], V. V. Dudelev[b], L. Ya. Karachinsky[a,b,c], I. I. Novikov[a,b,c], D. V. Denisov[d], S. O. Slipchenko[b], A. V. Lyutetskii[b], N. A. Pikhtin[b], G. S. Sokolovskii[b], and A. Yu. Egorov[c]

[a] *Connector Optics LLC, St. Petersburg, 194292 Russia*
[b] *Ioffe Institute, St. Petersburg, 194021 Russia*
[c] *ITMO University, St. Petersburg, 197101 Russia*
[d] *Saint Petersburg Electrotechnical University "LETI", St. Petersburg, 197022 Russia*
**e-mail: a.babichev@mail.ioffe.ru*

Received February 12, 2020; revised February 12, 2020; accepted February 13, 2020

Abstract—The method of molecular-beam epitaxy was used to fabricate an elastically balanced heterostructure of a quantum-cascade laser for the spectral range of 4.6 μm based on a heteropair of solid alloys, $In_{0.67}Ga_{0.33}As/In_{0.36}Al_{0.64}As$, and indium phosphide layers serving as waveguide cladding layers. An X-ray diffraction analysis demonstrated the high uniformity of the composition and thickness of layers in cascades of the heterostructure over the substrate area. Lasers with four cleaved facets show lasing at room temperature at a wavelength close to 4.6 μm with a comparatively low threshold current density of 1.1 kA/cm^2.

Keywords: superlattices, quantum-cascade laser, epitaxy, indium phosphide.

DOI: 10.1134/S1063785020050028

The emission wavelength of quantum-cascade lasers (QCLs) for the spectral range of 3.5–4.8 μm falls within the first atmospheric transparency window, for which reason they are important in a number of applications, such as spectroscopy, gas analysis, medical diagnostics, and surgery. Because of the existence of an absorption band of CO_2 at wavelengths in the range 4.2–4.4 μm, the atmospheric transparency window is subdivided into two spectral subranges: 3.5–4.2 and 4.4–4.8 μm. The systems created on the basis of QCLs for the spectral range of 4.4–4.8 μm exhibit a higher reliability, compact size, and lower cost [1] than do systems based on gas-phase and solid-state lasers.

One reason why the efficiency of QCLs for the spectral range of 4.4–4.8 μm is limited is the thermal excitation of carriers from the upper quantum-confinement level into the continuous spectrum ("continuum"), resulting from the insufficient band offset at the $In_{0.53}Ga_{0.47}As/In_{0.52}Al_{0.48}As$ heterointerface [1]. This problem can be solved by using mechanically strained heteropairs [2, 3], active region designs with additional AlAs layers [4], and layers with various heights of potential barriers [5]. When the method of molecular-beam epitaxy is used, the latter two approaches require that additional metal sources should be used during the epitaxial process.

This Letter presents the results obtained with elastically balanced QCL heterostructures for the spectral range of 4.6 μm that were grown by the method of molecular-beam epitaxy and have an active region based on the $In_{0.67}Ga_{0.33}As/In_{0.36}Al_{0.64}As$ heteropair, as well as with QCLs on their basis.

The QCL heterostructure was grown by Connector Optics LLC on a Riber 49 industrial molecular-beam epitaxy system equipped with a solid-state arsenic source, phosphorus source of the cracker type, and ABI 1000 sources for creating flows of gallium and indium [6–8]. InP (001) wafers doped with sulfur to a level $n = 3 \times 10^{17}$ cm^{-3} served as a substrate. The 3-μm-thick indium phosphide layer doped with silicon to $n = 1 \times 10^{17}$ cm^{-3} served as the lower cladding layer of the waveguide. The active region included 30 cascades based on the solid alloy heteropair $In_{0.67}Ga_{0.33}As/In_{0.36}Al_{0.64}As$. According to theoretical estimates, using a mechanically strained $In_{0.67}Ga_{0.33}As/In_{0.36}Al_{0.64}As$ heteropair makes it possible to raise the conduction band offset at the heterointerface by 310–330 meV (to 800–820 meV) as compared with the mechanically unstrained $In_{0.53}Ga_{0.47}As/In_{0.52}Al_{0.48}As$ heteropair, which diminishes the "overbarrier" escape of carriers [6]. The thickness of $In_{0.67}Ga_{0.33}As/In_{0.36}Al_{0.64}As$ layers was chosen with consideration for the compensation of the

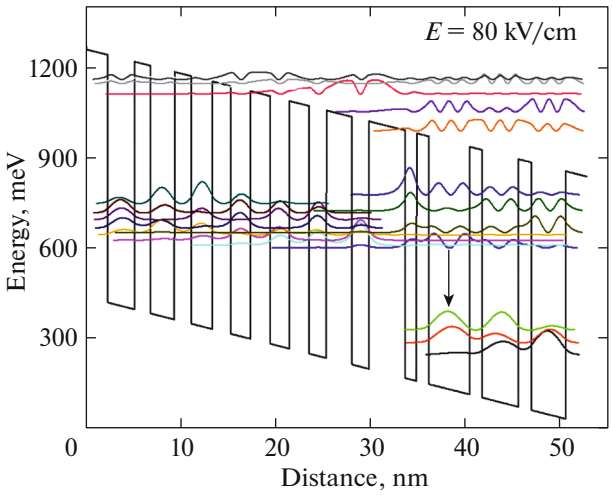

Fig. 1. Results of a numerical calculation of the conduction band profile and squared wave functions in the cascade layers of the active region at an electric field strength of 80 kV/cm.

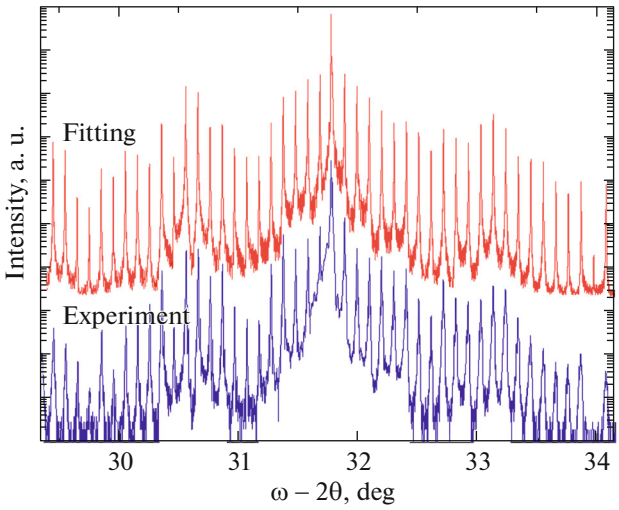

Fig. 2. XRD curve of the QCL heterostructure (lower curve) and the result of a numerical calculation (upper curve).

mechanical stress of layers in the cascade to form an elastically balanced heterostructure. The design of an active-region cascade is shown in Fig. 1. Together with the conduction band profile, the figure presents the squared wave functions in the layers of the cascade of calculated design, with two-phonon resonant scattering of carriers [9]. The arrow in Fig. 1 shows the radiative transition with photon energy of 271 meV, which corresponds to the wavelength of 4.57 μm. The total thickness of layers in a cascade was 50.4 nm. The upper cladding layer of the waveguide was formed on the basis of indium phosphide layers with thicknesses of 2 and 1 μm and doping levels of 1×10^{17} and 2×10^{19} cm^{-3}, respectively. The contact layer was a 200-nm-thick $In_{0.53}Ga_{0.47}As$ layer doped to 2.5×10^{19} cm^{-3}.

The structural perfection of the heterostructure was evaluated and the layer thicknesses in the cascades estimated by X-ray diffraction (XRD) analysis. XRD spectra were measured near the symmetric (004) reflection of InP with a PANalytical X'Pert Pro diffractometer in the parallel X-ray beam configuration [3, 10]. Figure 2 shows an experimental rocking curve measured at the center of the wafer (lower curve), together with the results of a numerical simulation. The XRD curve shows that the zero peak of the satellite structure completely coincides with the peak from the InP substrate. This fact indicates that the chemical composition of the epitaxial layers precisely corresponds to the prescribed values presented in the growth specification. The rocking curve shows 49 satellite peaks characteristic of the periodic structure of the cascades. Analysis of the curve gives a rather small full width at half-maximum (FWHM) of the satellite peaks (16″ ± 2″), compared with the previously reported results (29″–40″) [11–13], which is indicative of a high uniformity of the composition and thicknesses of various cascades in the heterostructure obtained. The positions of 24 satellite peaks were used to estimate the average cascade thickness to be 50.4 ± 0.6 nm. The XRD curves were also measured at distance of 14 mm from the substrate center. According to the simulation results, the deviation of the average thickness of the cascades does not exceed 0.4% from that at a substrate center, which is indicative of a high uniformity of the layers over the heterostructure surface. Thus, the XRD data indicate that the heterostructure has a high structural perfection and the thicknesses and compositions of the layers in the cascades fully correspond to those in the growth specification.

To examine the electroluminescent properties, we formed QCLs with four cleaved facets and a (390 × 500) ± 18-μm metallic contact [3]. The samples were mounted with the epitaxial surface down on a copper heatsink. The spectral characteristics of the QCLs were examined under pumping with current pulses with a width of ~75 ns and repetition rate of 48 kHz on an MDR-23 monochromator with a 150-mm^{-1} diffraction grating. The heatsink temperature was stabilized at 15°C. The emission was recorded with a Vigo PVI-4TE-10.6 cooled photodetector with lock-in detection [14]. The spectral measurements demonstrated the existence of lasing near 4.6 μm (Fig. 3). Two optical modes are present in the lasing spectrum. The intermode spacing was 11.4 nm. The dependence of the integral emission intensity under pumping with current pulses with width of ~75 ns and repetition rate of 48 Hz is shown in Fig. 3. The threshold current was 2.2 A, which corresponds to a low threshold current

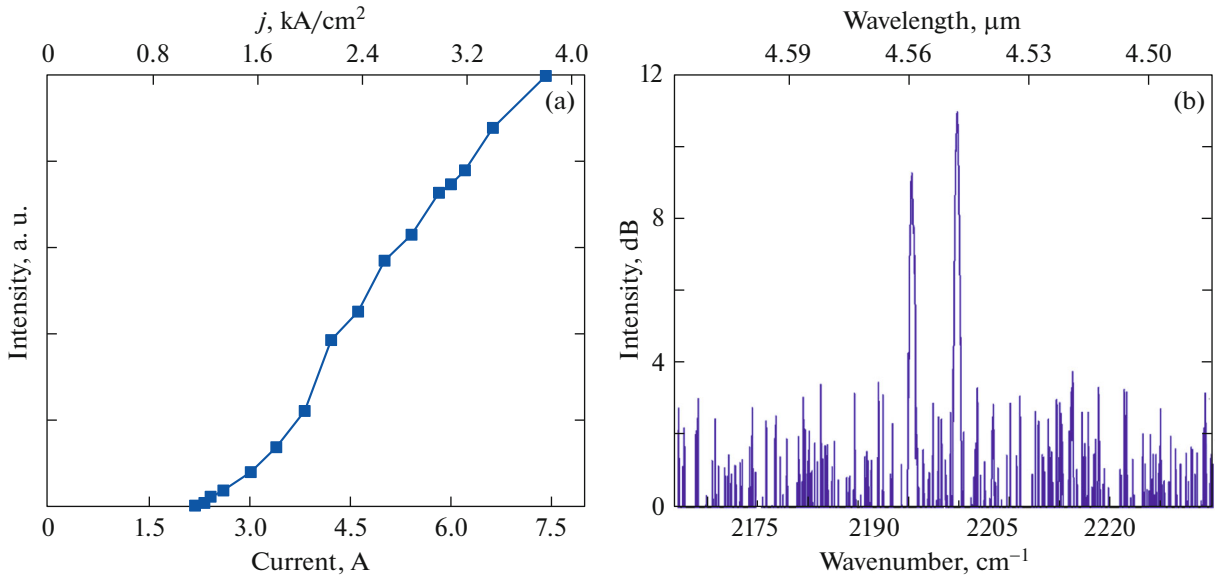

Fig. 3. (a) Dependence of the integral emission intensity on the drive current and (b) lasing spectrum of a QCL with four cleaved faces.

density (1.1 kA/cm^2). The threshold voltage of the lasers was 6 V.

As shown previously, the high modal gain (at the level of 3 cm/kA [15]) enables lasing in a QCL with four cleaved facets at room temperature [16] and a high output optical power in ridge-geometry lasers at the level of 1 W from a facet [17].

The lasing of a QCL with four cleaved facets at room temperature with low threshold current density is indicative, in comparison with the data of [16], of a high modal gain of the active region of the heterostructure and of the prospects for use of this class of heterostructures based on a mechanically strained $In_{0.67}Ga_{0.33}As/In_{0.36}Al_{0.64}As$ heteropair for continuous-wave lasing of QCLs for the 4.6-μm spectral range.

FUNDING

The study was supported by the Ministry of Science and Higher Education of the Russian Federation, unique project identifier RFMEFI60719X0318.

CONFLICT OF INTEREST

The authors declare that they have no conflict of interest.

REFERENCES

1. A. Lyakh, R. Maulini, A. Tsekoun, and R. Go, Proc. Natl. Acad. Sci. U. S. A. **107**, 18799 (2010). https://doi.org/10.1073/pnas.1013250107
2. M. Suttinger, R. Kaspi, and A. Lyakh, in *Mid-Infrared Optoelectronics: Materials, Devices, and Applications* (Woodhead, Cambridge, UK, 2020). https://doi.org/10.1016/b978-0-08-102709-7.00005-x
3. A. Yu. Egorov, A. V. Babichev, L. Ya. Karachinsky, I. I. Novikov, E. V. Nikitina, M. Tchernycheva, A. N. Sofronov, D. A. Firsov, L. E. Vorob'ev, N. A. Pikhtin, and I. S. Tarasov, Semiconductors **49**, 1527 (2015). https://doi.org/10.1134/s106378261511007x
4. M. Razeghi, W. Zhou, S. Slivken, Q.-Y. Lu, D. Wu, and R. McClintock, Appl. Opt. **56** (31), H30 (2017). https://doi.org/10.1364/ao.56.000h30
5. D. Botez, J. D. Kirch, C. Boyle, K. M. Oresick, C. Sigler, H. Kim, B. B. Knipfer, J. H. Ryu, D. Lindberg, T. Earles, L. J. Mawst, and Y. V. Flores, Opt. Mater. Express **8**, 1378 (2018). https://doi.org/10.1364/ome.8.001378
6. A. V. Babichev, A. G. Gladyshev, A. S. Kurochkin, E. S. Kolodeznyi, G. S. Sokolovskii, V. E. Bougrov, L. Ya. Karachinsky, I. I. Novikov, A. Bousseksou, and A. Yu. Egorov, Semiconductors **52**, 1082 (2018). https://doi.org/10.1134/s1063782618080031
7. A. V. Babichev, A. S. Kurochkin, E. S. Kolodeznyi, A. V. Filimonov, A. A. Usikova, V. N. Nevedomsky, A. G. Gladyshev, L. Ya. Karachinsky, I. I. Novikov, A. Yu. Egorov, and D. V. Denisov, Semiconductors **52**, 745 (2018). https://doi.org/10.1134/s1063782618060039
8. A. V. Babichev, G. A. Gusev, A. N. Sofronov, D. A. Firsov, L. E. Vorob'ev, A. A. Usikova, Yu. M. Zadiranov, N. D. Il'inskaya, V. N. Nevedomskii, V. V. Dyudelev, G. S. Sokolovskii, A. G. Gladyshev, L. Ya. Karachinsky, I. I. Novikov, and A. Yu. Egorov, Tech. Phys. **63**, 1511 (2018). https://doi.org/10.1134/s1063784218100043

9. D. Hofstetter, M. Beck, T. Aellen, and J. Faist, Appl. Phys. Lett. **78**, 396 (2001). https://doi.org/10.1063/1.1340865
10. A. V. Babichev, A. G. Gladyshev, D. V. Denisov, L. Ya. Karachinsky, I. I. Novikov, L. Boulley, A. Bousseksou, N. A. Pikhtin, and A. Yu. Egorov, Opt. Spectrosc. **127**, 279 (2019). https://doi.org/10.1134/s0030400x19080058
11. S. Slivken, A. Matlis, C. Jelen, A. Rybaltowski, J. Diaz, and M. Razeghi, Appl. Phys. Lett. **74**, 173 (1999). https://doi.org/10.1063/1.123284
12. A. V. Babichev, A. G. Gladyshev, A. V. Filimonov, V. N. Nevedomskii, A. S. Kurochkin, E. S. Kolodeznyi, G. S. Sokolovskii, V. E. Bugrov, L. Ya. Karachinskii, I. I. Novikov, A. Bousseksou, and A. Yu. Egorov, Tech. Phys. Lett. **43**, 666 (2017). https://doi.org/10.1134/s1063785017070173
13. A. V. Babichev, A. G. Gladyshev, A. S. Kurochkin, E. S. Kolodeznyi, V. N. Nevedomskii, L. Ya. Karachinsky, I. I. Novikov, A. N. Sofronov, and A. Yu. Egorov, Semiconductors **53**, 345 (2019). https://doi.org/10.1134/s1063782619030023
14. V. V. Dyudelev, S. N. Losev, V. Yu. Myl'nikov, A. V. Babichev, E. A. Kognovitskaya, S. O. Slipchenko, A. V. Lyutetskii, N. A. Pikhtin, A. G. Gladyshev, L. Ya. Karachinskii, I. I. Novikov, A. Yu. Egorov, V. I. Kuchinskii, and G. S. Sokolovskii, Opt. Spectrosc. **125**, 402 (2018). https://doi.org/10.1134/s0030400x18090096
15. A. V. Babichev, D. A. Pashnev, A. G. Gladyshev, A. S. Kurochkin, E. S. Kolodeznyi, L. Ya. Karachinskii, I. I. Novikov, D. V. Denisov, V. V. Dyudelev, D. A. Firsov, L. E. Vorob'ev, S. O. Slipchenko, A. V. Lyutetskii, N. A. Pikhtin, and A. Yu. Egorov, Opt. Spectrosc. (in press).
16. A. V. Babichev, A. G. Gladyshev, E. S. Kolodeznyi, A. S. Kurochkin, G. S. Sokolovskii, V. E. Bougrov, L. Ya. Karachinsky, I. I. Novikov, V. V. Dudelev, V. N. Nevedomsky, S. O. Slipchenko, A. V. Lutetskiy, A. N. Sofronov, D. A. Firsov, L. E. Vorobjev, and N. A. Pikhtin, J. Phys.: Conf. Ser. **1124**, 041029 (2018). https://doi.org/10.1088/1742-6596/1124/4/041029
17. V. V. Dudelev, D. A. Mikhailov, A. V. Babichev, A. D. Andreev, S. N. Losev, E. A. Kognovitskaya, Yu. K. Bobretsova, S. O. Slipchenko, N. A. Pikhtin, A. G. Gladyshev, D. V. Denisov, I. I. Novikov, L. Ya. Karachinsky, V. I. Kuchinskii, A. Yu. Egorov, and G. S. Sokolovskii, Quantum Electron. **50**, 141 (2020). https://doi.org/10.1070/QEL17168

Translated by M. Tagirdzhanov